Two hybrid directivity models of muzzle blasts to describe the frequency and distance dependency

Philipp Bechtel
Cervus Consult GmbH

Christian Kleinhenrich
Cervus Consult GmbH

Karl-Wilhelm Hirsch
Cervus Consult

TWO HYBRID DIRECTIVITY MODELS OF MUZZLE BLASTS TO DESCRIBE THE FREQUENCY AND DISTANCE DEPENDENCY

Philipp Bechtel* **Christian Kleinhenrich** **Karl-Wilhelm Hirsch**
Cervus Consult GmbH, Germany

ABSTRACT

The muzzle blast is an auditory risk if the shooter or other personnel are exposed close to the weapon. To evaluate the risk, the signature of the blast must be measured or synthesized for simulation purposes. Muzzle blasts are highly directional. A common approach for simulation is to assume a source model with scalar directivity. This approach neglects the angle- and distance-dependent changes in the frequency spectrum of the blast. Hence, significant discrepancies occur between synthesized and measured shooting signals. This paper presents two alternative approaches to describe the distance- and frequency-dependent directivity of a muzzle blast. The first approach is based on the ANX model by Salomons. In contrast to the scalar directivity of the latter, here a separate source energy is determined for each exit angle using cosine transformation. This model synthesizes the blasts with only a few parameters. For the second model, a transfer function is given by the ANX model and a spherical harmonic source describes the angle and frequency dependency of the blast signature. Depending on the input data, this model provides very detailed reconstructions of measured muzzle blasts even close to the muzzle.

Keywords: *Muzzle blasts, nonlinear, directivity, ANX*

1 INTRODUCTION

The hearing load of the shooter when firing handguns is primarily caused by the muzzle blast. The decisive input variable of models for assessing the exposure and the risk of hearing damage is the sound pressure time curve at the ear. For the investigation of such exposure models, reliable source models of the muzzle blast are required, which provide the sound pressure time signal. In addition to the pronounced frequency-dependent directivity of the muzzle blast, nonlinear effects in sound propagation must be taken into account in the near field of the weapon.

2 FUNDAMENTELS: DIRECTIVITY OF A MUZZLE BLAST

First, the special features of the directivity of a muzzle blast are discussed.

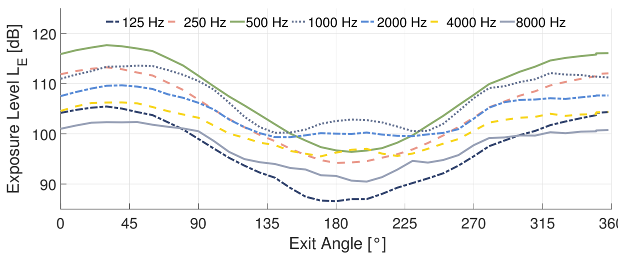

(a) Gun muzzle blast

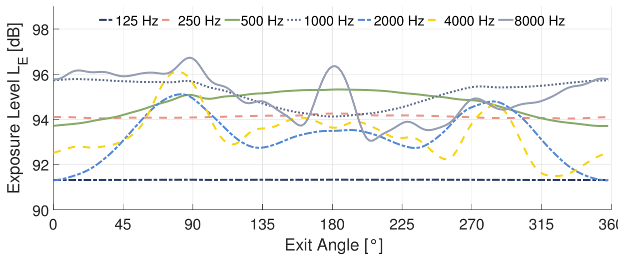

(b) Loudspeaker

Figure 1: Level of octave bands as a function of the exit angle in the transversal plane for a gun muzzle blast and a loudspeaker (Genelec 8020c)

The level deviations of the octave bands over the azimuth

**Corresponding author*: *bechtel@cervus.de*

angle in the transversal plane of a rifle muzzle blast and a loudspeaker are shown in Figure 1. Measurement data from the Genelec 8020c from the BRAS project was used for the loudspeaker directivity[1]. The following aspects become clear from the comparison of the level deviations of the octave bands.

- The octave band-dependent level deviation of the muzzle blast is up to 20 dB depending on the angle of exit and is therefore many times greater than that of the loudspeaker
- The eccentricity - the level difference between the front (firing direction) and the rear - of the muzzle blast is most pronounced in the low frequency bands of 125 Hz to 500 Hz and decreases towards high frequencies from approximate 20 dB to 10 dB
- Most of the energy of this rifle is emitted between 500 Hz and 1 kHz

The propellant gases escaping from the tube during the muzzle blast resemble a massively deformed sphere, as indicated in the schlieren photography from Figure 2.

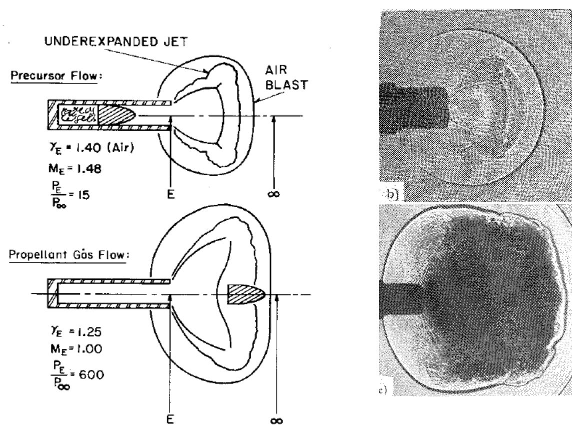

Figure 2: Flows occurring during the muzzle blast[2]

The first spherical sound front recognizable in the schlieren photography is the so-called *precursor*, which originates from the air pushed out by the projectile at supersonic speed. The actual muzzle blast is formed by the propellant gases behind the projectile. These also emerge from the pipe at supersonic speed and flow into the still air. This forms a so-called Mach plate, a well-known phenomenon in fluid dynamics[2]. The muzzle blast is therefore emitted neither from the muzzle itself nor from a sphere around it, but from a disk[3]. This explains why the directional effect is also directed forwards at longer wavelengths, while it tends to remain round at shorter wavelengths.

3 RAW AND REFERENCE DATA

In Figure 3 the 36 measuring points are outlined in the horizontal plane.

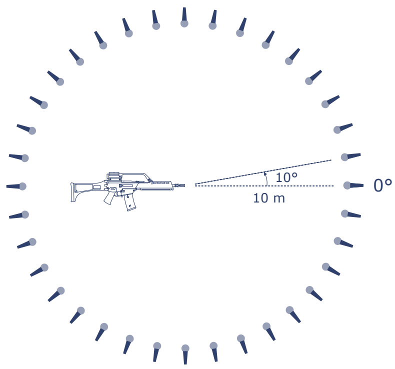

Figure 3: Sketch of the 360° measurement

There are three recorded shot signals per measuring point. The distance between the microphones and the muzzle is 10 m. The weapon used is a rifle on a fixture with a muzzle brake [1] . Both the muzzle and the respective measuring points are positioned 2 m above the approximately reverberant grass ground. This means that the ground reflection hits approximate 2.1 ms after the direct sound. For the investigations presented here, only the direct sound component windowed out using Hamming windows is considered. The full metal jacket ammunition corresponds to the caliber 5.56 mm × 45 mm. In the calculations, an exit velocity v_0 = 1200 $^m/_s$ and a projectile mass m_p = 3.7 g were assumed for this ammunition.

A total of six additional measurement points from another measurement campaign were used to investigate the propagation models. There, the same rifle type with identical ammunition was measured on an open shooting range. In contrast to the 360° measurement, the ground here consisted of gravel and a shooter was used instead of a fixture. Four of the six reference points are outlined in Figure 4.

[1] According to the current state of the investigation, the muzzle brake influences the emitted sound from an angle of ≈ 140°, so that no clean blast is measured there.

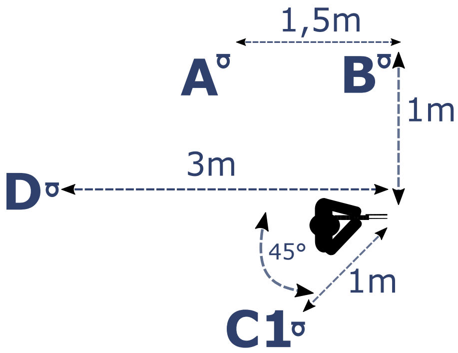

Figure 4: Sketch of reference measuring points

The two remaining measuring points C5 and C10 are in the propagation path of measuring point C1 at a distance of 5 m and 10 m from the muzzle.

4 ANX SOURCE MODEL

This model was introduced in 2024 by Salomons[4] under the title: *Analytical model for sound of explosives and firearms (ANX)*. It is based on a Friedlander blast[5], which has two characteristic values with the peak sound pressure P and the positive transit time T. The characteristic values and the resulting sound pressure time curve are sketched in Figure 5.

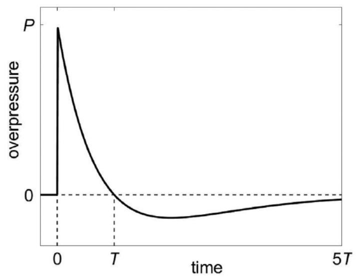

Figure 5: Friedlander waveform, with peak sound pressure P and positive transit time T[4]

The special feature of the ANX model is the nonlinear sound propagation. Here, the peak sound pressure $P(r)$ and the duration of the positive N-wave flank $T(r)$ are distance-dependent variables that are determined according to Equations (2) and (3). As the spectral energy of a signal moves increasingly towards low frequencies with increasing $T(r)$, a blast becomes more low-frequency

Table 1: Relevant constants and reference values

K	β	ρ	c	t_0	p_0
0.38	1.2	1.2 $^{kg}/_{m^3}$	340 $^{m}/_{s}$	1 s	20 µPa

with increasing distance from the muzzle according to the ANX model.

The auxiliary variable r_*, which depends on the source energy E, limits the application range of the model with $r > 1.6\, r_*$ and can be determined according to Equation (4) with the values from Table 1. The source energy of handguns is usually less than 20 kJ which corresponds to a maximum r_* of 367 mm. This means that the model is suitable for most handguns from a distance of approximately 0.6 m applicable.

$$p(t) = P(r)\left(1 - \frac{t}{T(r)}\right) e^{-t/T(r)} \tag{1}$$

$$P(r) = K\rho c^2 \frac{r_*}{r} \sqrt{\frac{1}{\ln(^r/_{r_*})}} \tag{2}$$

$$T(r) = K\beta \frac{r_*}{c} \sqrt{\ln(\frac{r}{r_*})} \tag{3}$$

$$r_* = 0.7 \sqrt[3]{\frac{E}{\rho c^2}} \tag{4}$$

4.1 Scalar directivity

Salomons[4] uses a scalar approach with the directivity D. This value can be calculated with the reference quantity $m_0 = 75$ g according to Equation (5). For small arms, the propellant mass m is only a few grams, so that $m \ll m_0$ applies and the directivity is approximately 17.5 dB. The directional correction term C_{dir} can be determined according to Equation (6) and is for $m \ll m_0$ approximately 11 dB.

The scalar, exit angle-dependent correction level $\Delta L(\phi)$ thus results in Equation (7).

$$D = \frac{17.5}{1 + (^m/_{m_0})^{1.5}} \tag{5}$$

$$C_{\text{dir}} = 10 \log \left(\frac{10}{D} \frac{10^{D/10}}{\ln(10)} \left[1 - 10^{-D/10} \right] \right) \quad (6)$$

$$\Delta L(\phi) = D \left(1 - \frac{\phi}{180} \right) - C_{\text{dir}} \quad (7)$$

For the rifle considered here, the source energy $E = 2500\,\text{J}$ is assumed.

4.2 Source energy-dependent directivity by cosine transformation

In this approach, an angle-dependent source energy $E(\phi)$ is determined. Using the coefficients of a rifle of 5.56 mm × 45 mm caliber from Table 2, the angle-dependent source energy can be determined by cosine transformation according to Equation (8). The angle-dependent source energy can then be used to calculate the distance-dependent signal parameters according to Equations (2) and (3) from which the final signals at the receiver result.

Table 2: Coefficients for determining the direction-dependent source energy of a rifle muzzle blast using the 5th order cosine transformation

Index i	1	2	3	4	5
c_i / J	2521	1908	557	79	52

$$E(\phi) = \sum_{i=1}^{N} c_i \cdot cos(\phi \cdot (i-1)) \quad (8)$$

5 SPHERICAL HARMONICS (SH) SOURCE

As a further source model, a transformation of the measurement data into the spherical frequency domain is considered. This was carried out with a 15th order spherical harmonics decomposition, resulting in 256 complex coefficients for each frequency support point. The method is described in more detail by Williams[6], among others. The reconstructed signals of this source model naturally only represent this type of rifle with the corresponding ammunition.

6 PROPAGATION MODELS

This chapter deals with two different propagation models. Both deal exclusively with distance-dependent attenuation. For example, atmospheric attenuation components that also occur during sound propagation are not taken into account in these models.

The reference distance r_0 was used for the spherical harmonics 10 m, as the data used for the decomposition was available at this distance. For the ANX source model, $r_0 = 1$ m was selected as the reference distance.

6.1 Linear sound propagation model

The linear propagation model uses the $1/r$ approach commonly used in acoustics. The calculation of the sound pressure time curve $p_r(t, \phi)$ at a distance r is shown in Equation (9), neglecting the phase and other attenuation effects.

$$p_r(t, \phi) = p_{r_0}(t, \phi) \cdot \frac{r_0}{r} \quad (9)$$

6.2 Nonlinear sound propagation model

This model describes the nonlinear sound propagation of an N-wave with spherical expansion in a homogeneous environment according to Pierce[7] [2]. The implementation of this model is based on the ANX model according to Section 4.

To determine the distance-dependent transfer function, the angle-dependent energy $E(\phi)$ of the sound source is first required. If this is not available, but for example sound pressure time curves at the known source distance r, the energy of these signals can be estimated. To do this, the exposure level L_E of the signal must be calculated. From this level, the auxiliary variable r_* can then be estimated according to Equation (10) [3]. With the constants and reference quantities from Table 1, the source energy can finally be determined with Equation (11).

$$L_E = 10 \log \left(\frac{\pi K^3 \beta \rho^2 c^3 r_*^3}{p_0^2 r_0^2 t_0} \frac{r_0^2}{4\pi r^2} \sqrt{\frac{1}{\ln(r/r_*)}} \right) \quad (10)$$

[2] Chapter 11.9

[3] According to Salomons[4], the deviation is less than 1 dB

$$E = \rho c^2 \left(\frac{r_*}{0.7}\right)^3 \tag{11}$$

In the next step, the creation of the transfer function is outlined. The angle-dependent source energy $E(\phi)$ is used to generate an ANX signal $p_{r_0}(t,\phi)$ for the reference distance r_0 and a second signal $p_r(t,\phi)$ for the desired source distance r. Using Fourier transformation, these two signals are transferred to the frequency domain and the quotient is formed, which corresponds to the transfer function.

By multiplying the source signal, which has also been transformed into the frequency domain, with the transfer function, the frequency response of the signal at a distance r at the angle of exit ϕ can be determined. The back transformation into the time domain results in the shot signal at the observation point with nonlinear sound propagation.

7 INVESTIGATION

In this section, the source models presented are examined with regard to their applicability in the vicinity of the muzzle. For this purpose, the predicted hearing load as well as the sound pressure time curves and frequency responses are considered.

Table 3: Nomenclature of the abbreviations

Scalar Directivity	scalar directivity according to Section 4.1
Cosine Trans.	energetic directivity according to Section 4.2
Linear	linear propagation model according to Section 6.1
NL	nonlinear propagation according to Section 6.2

The abbreviations used in the following can be taken from Table 3.

7.1 Predicted hearing load

The AHAAH model[8] used to determine the hearing load was developed explicitly for shooting noise. It is an appropriate hearing damage prediction method and is currently used by the US military[9], among others. The AHAAH settings unwarned, no hearing protection and frontal sound incidence were used consistently for all calculations.

The following statements can be derived from the hearing loads presented in Figure 6 over the angle of exit at a distance of 10 m.

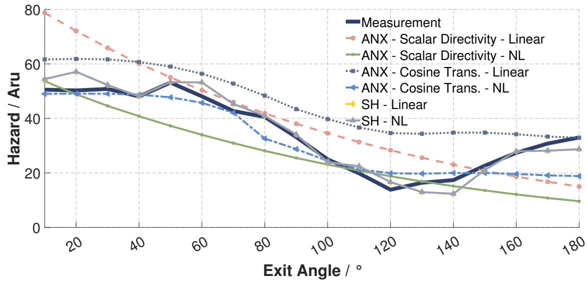

Figure 6: Hearing load over the angle of exit in 10 m muzzle distance

- The predicted hearing load of the measurement signals decreases with increasing angle until the influence of the muzzle brake from $\approx 140°$ causes it to increase again
- The curves of the spherical harmonics reconstructions with linear and nonlinear sound propagation are identical due to the reference distance $r_0 = 10$ m and deviate only slightly from the target values
- The hearing loads according to the ANX models with scalar directivity decrease approximately linearly over the angle of exit. As expected, the values are higher with the linear propagation model, as both the stronger additional level drop and the shift in the spectrum are neglected. The correlation with the values of the measurement are only low for the ANX source models with scalar directivity
- The ANX source model with cosine transformation directivity significantly overestimates the target values in a linear propagation calculation. In combination with the nonlinear propagation model, the method provides appropriate hearing exposure predictions for angles $< 140°$

Next, the models are analysed on the reference data according to Figure 4. For this purpose, Figure 7 shows the hearing loads at the reference measuring points removed in 1 m to 10 m and the following statements can be derived.

- The predicted hearing load of the measurement signals tends to decrease with increasing distance to the muzzle
- At the measurement points B and C1 near the muzzle, the spherical harmonics values deviate significantly from each other depending on which propagation

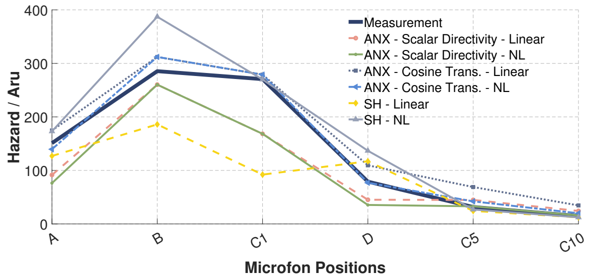

Figure 7: Hearing load at the reference measuring points according to Figure 4

method was used. The deviations with the nonlinear propagation model are significantly lower compared to the target values

- The ANX model with scalar directivity significantly underestimates the actual hearing load for the most part, regardless of the propagation model
- The ANX source model with the cosine transformation directivity and nonlinear sound propagation provides almost identical hearing damage risk as the measurement data When using the linear propagation model, the overestimation of the hearing load increases with the distance to the muzzle

7.2 Reconstructed shot signals

For further investigation, the measured and reconstructed signals at two measuring points on the circle after Figure 3 as well as two relevant positions at 1 m muzzle distance are considered in more detail.

In Figures 8 and 9 the sound pressure time curves and frequency responses at two representative measurement points of the circular measurement are discussed. This shows that, as expected, the spherical harmonics signals are identical to each other and show hardly any deviations from the measurement signals. The ANX approaches with linear sound propagation significantly overestimate the peak levels, in some cases by more than 6 dB. With the nonlinear propagation model, the differences to the target values are significantly smaller. With regard to the frequency responses, all the source models considered provide reasonable reconstructions.

In Figures 10 and 11 the sound pressure time curves and frequency responses are discussed in 1 m distance at different exit angles. For the spherical harmonics signals, the

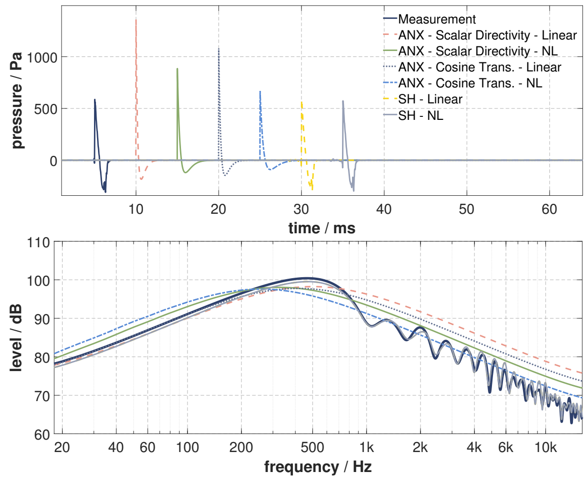

Figure 8: Sound pressure time curve and frequency response under 10° at 10 m distance

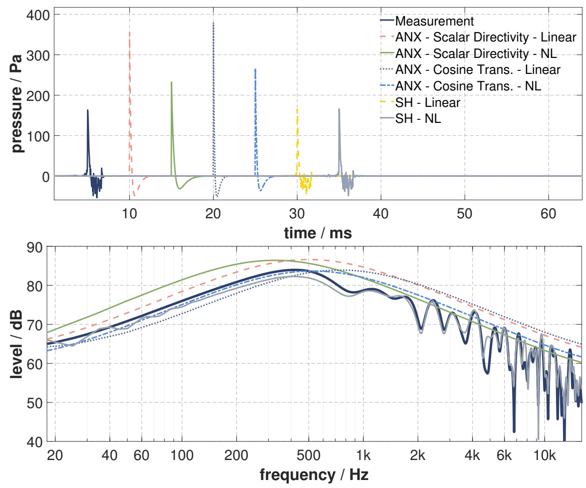

Figure 9: Sound pressure time curve and frequency response under 130° at 10 m distance

difference between them is 3 dB to 4 dB. The sound pressure time curves with nonlinear propagation tend to show higher similarities with the measured data. For the spectra, the model with nonlinear sound propagation also depicts the frequency responses above approx. 500 Hz better. Due to the short useful signal length of 7 ms, the curves below 500 Hz are only partially reliable.

As expected, the ANX source models show no differences at this distance with regard to the sound propagation method. In terms of directivity, the peak levels of the

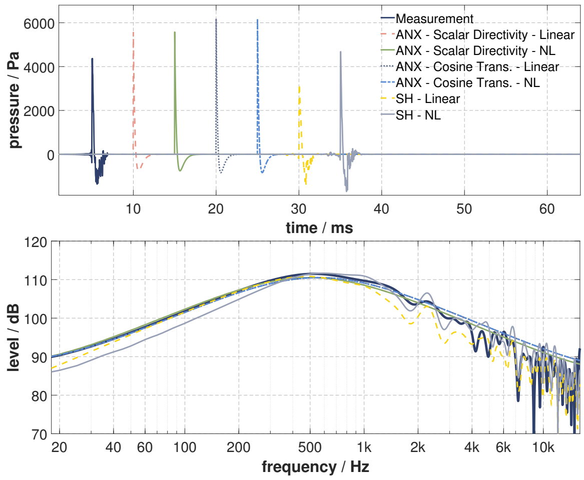

Figure 10: Sound pressure time curve and frequency response under 90° at 1 m distance (reference measuring point B)

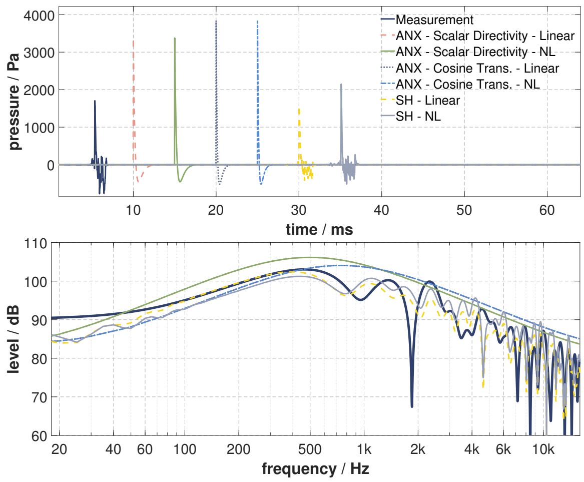

Figure 11: Sound pressure time curve and frequency response under 135° at 1 m distance (reference measuring point C1)

cosine transform method are slightly higher than those of the scalar approach. In addition, the spectra of the scalar ANX model are lower-frequency than those of the cosine transformation. Both ANX source models overestimate the peak level of the measurement signals with 3 dB to 8 dB, in some cases enormously. On closer inspection of the spectra, this difference results primarily from the overestimation of the frequency components above $\approx$ 3 kHz. The sound pressure time curves at measurement point B shown in Figure 12 were filtered low-pass [4] at 4 kHz for illustration purposes. A comparison with Figure 10 shows that the peak level differences of the ANX models compared to the measurement signal have fallen from above 3 dB to less than 1 dB.

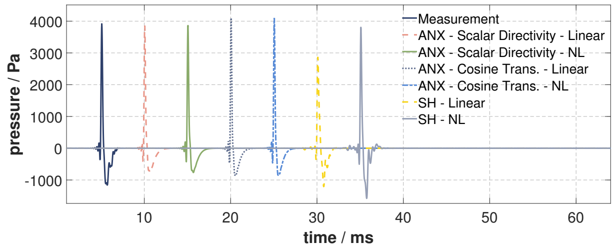

Figure 12: Low-pass [4] filtered sound pressure time curve under 90° at 1 m distance (reference measuring point B)

This aspect explains the high agreement of the AHAAH hearing damage predictions by the ANX model with cosine transformation and nonlinear propagation, despite the marked level differences. The reason for this lies in the way the AHAAH model works. This model calculates the auditory risk units for individual bark bands, whereby the maximum value is decisive. For the gunshot signals analysed here, the maximum ARU value is always in the frequency range between 1 kHz to 2.5 kHz. The lower and higher frequency signal components are therefore less significant when predicting the risk of hearing damage. Regardless of this, the ANX model tends to overestimate the energy of the high-frequency signal components of this gun muzzle blast, which requires further investigation.

8 CONCLUSION

It was shown that the ANX source model with cosine transformation as the directivity generates more realistic signals than the scalar approach, particularly with regard to the predicted hearing load. The reason for this lies in the oversimplified modelling approach of the frequency-dependent directivity of a muzzle blast. The attempt to model this with a single scalar factor logically results in higher deviations than with the more complex cosine transformation approach.

It also became clear that the quality of the shot signals generated close to the muzzle increases when nonlinear transfer functions are used instead of linear sound propa-

[4] 10th order Butterworth filter with 4 kHz cut-off frequency

gation. For example, the ANX model with cosine transform directivity and nonlinear propagation can be used to properly predict the hearing load of the direct sound component of the rifle muzzle blast, considered here as a function of both the angle of exit and the muzzle distance.

The results presented here are subject to some limitations. For example, only the direct sound components of gun blasts were considered. Investigations into the quality of the source and propagation models in combination with multiple reflections in closed systems are still pending. The fact that only one gun was considered here represents a further limitation. For further evaluation, the methods must be applied to other weapons and validated. As an alternative to the methods considered here, the Weber model is another source model to which the nonlinear sound propagation can be applied as a transfer function. Initial investigations into this appear promising.

9 ACKNOWLEDGMENTS

The work is supported by BAIUDBw GS II 2 and IUD I 5 of the German Ministry of Defense.

10 REFERENCES

[1] L. Aspöck, F. Brinkmann, D. Ackermann, S. Weinzierl, and M. Vorländer. *BRAS - Benchmark for Room Acoustical Simulation*. en. 2020. DOI: 10.14279/DEPOSITONCE-6726.3.

[2] E. M. Schmidt and D. D. Shearf. "Optical Measurements of Muzzle Blast". In: *AIAA Journal* 13.8 (1975), pp. 1086–1091.

[3] J. Zhang, G. Liu, W. Han, L. Liu, and Z. Wang. "Numerical research on the muzzle multiphase flow field produced by gas curtain launch". In: *Scientific Reports* 14.1 (Nov. 2024). ISSN: 2045-2322. DOI: 10.1038/s41598-024-81216-1.

[4] E. M. Salomons. "Analytical model for sound of explosives and firearms". In: *The Journal of the Acoustical Society of America* 156.3 (Sept. 2024), pp. 2034–2044. ISSN: 0001-4966. DOI: 10.1121/10.0030301.

[5] F. G. Friedlander. "The diffraction of sound pulses I. Diffraction by a semi-infinite plane". In: *Proceedings of the Royal Society of London. Series A. Mathematical and Physical Sciences* 186.1006 (Sept. 1946), pp. 322–344. ISSN: 2053-9169. DOI: 10.1098/rspa.1946.0046.

[6] E. G. Williams. *Fourier acoustics - Sound radiation and nearfield acoustical holography*. Academic Press, 1999. DOI: 10.1016/B978-0-12-753960-7.X5000-1.

[7] A. D. Pierce. *Acoustics: An Introduction to Its Physical Principles and Applications*. Springer International Publishing, 2019. ISBN: 9783030112141. DOI: 10.1007/978-3-030-11214-1.

[8] P. D. Fedele, M. S. Binseel, J. T. Kalb, and G. R. Price. *Using the Auditory Hazard Assessment Algorithm for Humans (AHAAH) With Hearing Protection Software, Release MIL-STD-1474E*. Tech. rep. ARL-TR-6748. Army Research Laboratory, 2013.

[9] US Department of Defense. *MIL-STD-1474E: Design Criteria Standard Noise Limits*. Military Standard. 2015.